A Bus Energy Model for Deep Submicron Technology

Paul P. Sotiriadis and Anantha P. Chandrakasan, *Senior Member, IEEE*

Abstract—We present a comprehensive mathematical analysis of the energy dissipation in deep submicron technology buses. The energy estimation is based on an elaborate bus model that includes distributed and lumped parasitic elements that appear as technology scales. The energy drawn from the power supply during the transition of the bus is evaluated in a closed form. The notion of the transition activity of an individual line is generalized to that of the transition activity matrix of the bus. The transition activity matrix is used for statistical estimation of the power dissipation in deep submicron technology buses.

Index Terms—Buses, deep submicron, power reduction, transition activity, transition activity matrix, very large scale integration (VLSI).

I. INTRODUCTION

A SIGNIFICANT amount of the power dissipated in digital circuits is due to long buses [1], [2]. Accurate estimation of the power drawn by the buses is important since both peak and average power influence the optimization of the drivers and the repeaters. Even more, an energy estimation model supports the performance evaluation of the digital circuit as a whole and the evaluation of power reduction techniques, for example, charge recycling [3]–[7], coding for low power [8]–[11,] and low-swing interconnect [12]–[14].

Until recently, a very simple bus model has been used for analytical energy estimation. The bus lines have been modeled by lumped grounded capacitors of equal sizes. This simple model though is not adequate for deep submicron (DSM) technology buses. Technology scaling introduces new dependencies that are not captured by this traditional bus model. The lines cannot be regarded as decoupled lumped elements. Instead, the lines strongly interact with each other through parasitic capacitances and inductances. Significant work has been done in modeling DSM technology interconnect networks, for example, [15]–[23]. The coupled dynamics of the lines results in dependencies between the energies drawn from the power supply by their drivers. This coupling due to interline parasitics becomes stronger with technology scaling, and in most cases, it is more significant than the coupling between individual lines and ground.
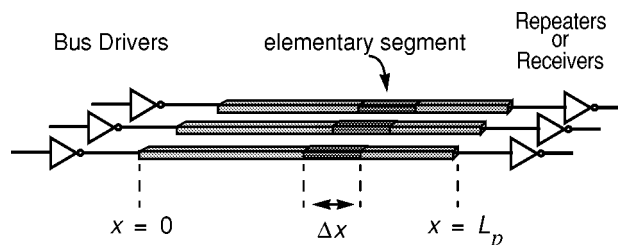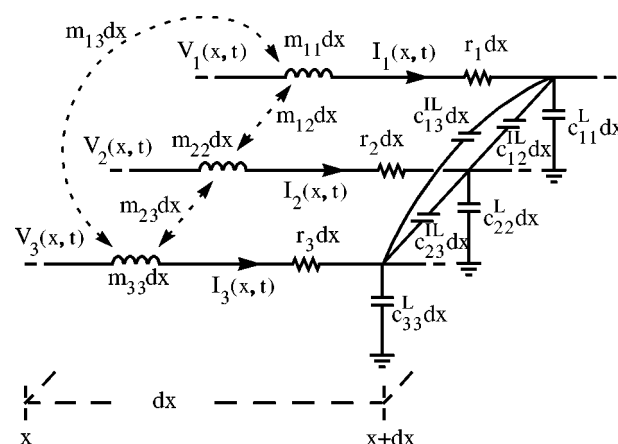
Fig. 1.   DSM bus.

Fig. 2.   Elementary segments of DSM bus lines.

The purpose of this paper is to present a compact energy model for DSM buses based on a detailed distributed circuit model. Similar work for the case of one line has been presented in [24].

II. DSM BUS MODEL

In general, a bus may consist of one set of parallel lines or more with repeaters between them. Here, we examine the simple case of one set of parallel lines driven by CMOS inverters and loaded by the input capacitors of the next stage as in Fig. 1. The energy for the general case is the sum of the energies of all stages.

A. Lines

For the DSM bus of Fig. 1, we will use the distributed line model of Fig. 2. The lines here are assumed distributed, lossy, capacitively, and inductively coupled. This is an established model for DSM bus lines. It has been used in the past for delay estimation as well as signal integrity evaluation [26]–[29].

The lines are laid along the x axis and have physical length L_p. All the major parasitic elements between lines and ground

(shielding or substrate) are included. The densities of the different quantities are $r_i(x)$ for the serial resistance of the ith line, $c_{i,i}(x)$ for the capacitance between the ith line and ground, and $c_{i,j}(x)$ for the capacitance between lines i and j. Also, $\mu_{i,i}(x)$ is the density of the self inductance of the ith line, and $\mu_{i,j}(x)$ is the density of the mutual inductance between lines i and j. The densities may depend on x. Finally, possible lumped parasitics can be included as limiting cases of distributed ones.

The current $I_i(x,t)$ is running through the ith line at the point $x \in [0, L_p]$ and time $t \geq 0$. Let $I = [I_1, I_2, \ldots, I_n]^T$ be the current vector. Similarly, $V_i(x,t)$ is the voltage of that point with respect to ground and let $V = [V_1, V_2, \ldots, V_n]^T$ be the voltage vector. The line model of Fig. 2 satisfies the system of partial differential equations

$$-\frac{\partial I}{\partial x}(x,t) = C(x)\frac{\partial V}{\partial t}(x,t) \tag{1}$$

and

$$-\frac{\partial V}{\partial x}(x,t) = M(x)\frac{\partial I}{\partial t}(x,t) + R(x)I(x,t). \tag{2}$$

The three $n \times n$ matrices R, M, C correspond to the distributed resistance, inductance, and capacitance, respectively. They have the following forms:

$$R(x) = \text{diag}[r_1(x), r_2(x), \ldots, r_n(x)] \tag{3}$$

[diagonal matrix with elements : $r_1(x), r_2(x), \ldots, r_n(x)$].

$$M(x) = [\mu_{i,j}(x)]_{i,j=1}^n \tag{4}$$

and

$$C(x) = C^L(x) + \sum_{i<j} C_{i,j}^{IL}(x). \tag{5}$$

The diagonal matrix

$$C^L(x) = \text{diag}[c_{1,1}^L(x), \ldots, c_{n,n}^L(x)] \tag{6}$$

corresponds to the parasitic capacitances between the lines and the ground. The matrices $C_{i,j}^{IL}, i < j$ correspond to the interline capacitance densities $c_{i,j}^{IL}(x)$. The matrix $C_{i,j}^{IL}(x)$ may have nonzero elements only in the entries $(i,i), (i,j), (j,i), (j,j)$ and it is of the form

$$C_{i,j}^{IL}(x) = c_{i,j}^{IL}(x) \begin{bmatrix} 0 & \cdots & 0 & \cdots & 0 & \cdots & 0 \\ \vdots & & \vdots & & \vdots & & \vdots \\ 0 & \cdots & 1 & \cdots & -1 & \cdots & 0 \\ \vdots & & \vdots & & \vdots & & \vdots \\ 0 & \cdots & -1 & \cdots & 1 & \cdots & 0 \\ \vdots & & \vdots & & \vdots & & \vdots \\ 0 & \cdots & 0 & \cdots & 0 & \cdots & 0 \end{bmatrix}. \tag{7}$$

As defined, $C(x)$ is the distributed capacitance conductance matrix of the lines.

So far, the electrical characterization of the bus lines has been given. More details can be found in the literature, for example, in [15], [19], and [22].

B. Timing Issues

Independently of the particular application, the data is expected to travel through the bus within some time period T. Without loss of generality, we can examine the bus during the time interval $[0, T]$. At $t = 0$, the bus is driven with the new data and at $t = T$ the data is sampled at the other end. It is reasonable to assume that by the time the data are sampled, the voltages along the lines have settled to their final values. In other words, if V_i^f is the data being transmitted through the ith line (V_i^f is 0 or V_{dd}), then after time T we have that

$$V_i(x, T) = V_i^f \tag{8}$$

for all $x \in [0, L_p]$ and $i = 1, 2, \ldots, n$ (superscript f stands for final). This assumption also implies that when the transition of the bus starts at time $t = 0$, the voltages along the lines correspond to their previous binary values

$$V_i(x, 0) = V_i^i \tag{9}$$

for all $x \in [0, L_p]$ and $i = 1, 2, \ldots, n$ (superscript i stands for initial). Relations (8) and (9) are the initial and final conditions of the system of partial differential equations (P.D.E.s) given by (1) and (2). For convenience, we define the vectors of initial and final voltages as, $V^i = \left[V_1^i, V_2^i, \ldots, V_n^i\right]$ and $V^f = \left[V_1^f, V_2^f, \ldots, V_n^f\right]$, respectively. Our assumption can be written as

$$V(x, 0) = V^i \tag{10}$$

and

$$V(x, T) = V^f \tag{11}$$

for all $x \in [0, L_p]$.

The dynamics of the bus lines along with their initial and final conditions are given by (1), (2), (10), and (11). We also need boundary conditions for the P.D.Es. These will be provided by circuit models for the drivers and the loads of the lines.

C. Drivers and Loads

Fig. 3 shows the ith line connected to its driver and load. The driver (CMOS inverter) has been modeled as a switch connecting the line either to the power supply or the ground through
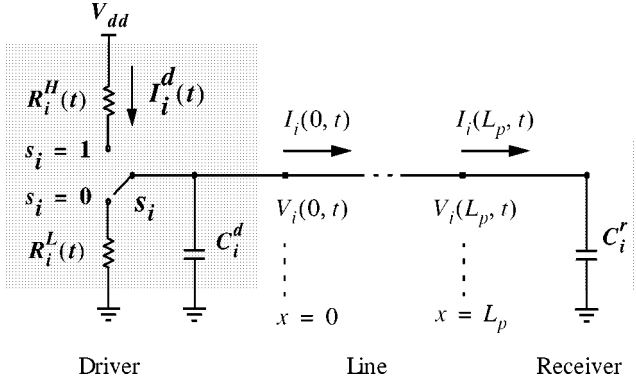
Fig. 3. Driver-line-receiver.

Fig. 4. Equivalent capacitive network ($n = 4$).

resistors [25].[1] The resistors $R_i^H(t)$ and $R_i^L(t)$ corresponding to the PMOS and NMOS transistors of the inverter are not necessarily the on resistors of the transistors in their linear regions. Their values can be *arbitrary* functions of time as long as the timing assumptions of Section II-B remain valid. The resistors simply express the current flow through the MOSFETs. The switch s_i connects to $R_i^H(t)$, ($s_i = 1$), or $R_i^L(t)$, ($s_i = 0$), depending on the binary value to be transmitted, i.e., depending on whether it is $V_i^f = V_{dd}$ or $V_i^f = 0$. Therefore, it is $V_i^f = s_i V_{dd}$. The capacitance C_i^d is the parasitic capacitance at the output of the ith driver. We define the diagonal matrix

$$C^d = \mathrm{diag}[C_1^d, C_2^d, \ldots, C_n^d]. \tag{12}$$

At the end of the line, the load (input of the receiver circuit) is represented by the capacitor C_i^r. We set

$$C^r = \mathrm{diag}[C_1^r, C_2^r, \ldots, C_n^r]. \tag{13}$$

In Fig. 3, $V_i(0, t)$ and $V_i(L_p, t)$ are the boundary voltages of the line. The currents $I_i(0, t)$ and $I_i(L_p, t)$ are the driving and loading currents of the line. The current drawn from V_{dd} is denoted by $I_i^d(t)$. This current is responsible for the power drawn from V_{dd} by the ith driver. The current is zero when $s_i = 0$. Even more, since $V_i^f / V_{dd} = s_i$, we can write

$$I_i^d(t) = \frac{V_i^f}{V_{dd}} \left\{ I_i(0, t) + C_i^d \frac{\partial V_i(0, t)}{\partial t} \right\} \tag{14}$$

for all $i = 1, 2, \ldots, n$.
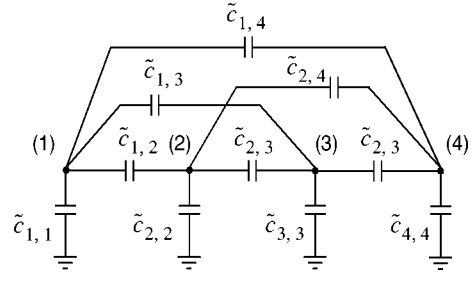
III. TRANSITION ENERGY

The energy drawn from V_{dd} by the ith driver during the transition period $[0, T]$ is given by

$$E_i = \int_0^T V_{dd} I_i^d(t) dt. \tag{15}$$

The time integral is evaluated in Appendix A and the energy E_i is given by the expression

$$E_i = V_i^f e_i^T C^t (V^f - V^i). \tag{16}$$

[1] This model does not account for the short-circuit currents of the drivers, which have to be evaluated independently using information of the waveforms in the inputs of the drivers.

The vector e_i has a one in the ith position and zero everywhere else. The matrix C^t, which we call the *total capacitance conductance matrix*, is given by the sum

$$C^t = C^d + C^r + \int_0^{L_p} C(x) dx \tag{17}$$

with C^d and C^r defined by (12) and (13), respectively, and the matrix function $C(x)$ given by (5). We define $\tilde{c}_{i,j}, i \neq j$ to be the total capacitance between lines i and j, ($\tilde{c}_{i,j} = \tilde{c}_{j,i}$), and $\tilde{c}_{i,i}$ to be the total capacitance between line i and ground (including the capacitances of the driver and the receiver). It is

$$\tilde{c}_{i,j} = \int_0^{L_p} c_{i,j}^{IL} dx \tag{18}$$

$$\tilde{c}_{i,i} = C_i^d + C_i^r + \int_0^{L_p} c_{i,i}^L dx. \tag{19}$$

We conclude that $C^t = \left[c_{i,j}^t \right]_{i,j=1}^n$ is the conductance matrix of the *lumped* capacitive network in Fig. 4 ($n = 4$ for simplicity). Even more, it is

$$c_{i,j}^t = \begin{cases} \sum_{k=1}^n \tilde{c}_{i,k}, & \text{if } i = j \\ -\tilde{c}_{i,j}, & \text{if } i \neq j. \end{cases} \tag{20}$$

By expanding the right part of (16), we have that the energy drawn from V_{dd} during the transition is

$$\begin{aligned} E_i &= V_i^f e_i^T C^t (V^f - V^i) \\ &= V_i^f (V_i^f - V_i^i) c_{i,i}^t + \sum_{j, j \neq i} V_i^f (V_j^f - V_j^i) c_{i,j}^t \\ &= V_i^f (V_i^f - V_i^i) \sum_{j=1}^n \tilde{c}_{i,j} - \sum_{j, j \neq i} V_i^f (V_j^f - V_j^i) \tilde{c}_{i,j}. \end{aligned} \tag{21}$$

We notice that this is exactly the energy that would be drawn from the power supply by the ith driver during the transition if the lines of the bus and the parasitic capacitances of the drivers and the receivers were replaced by the network of Fig. 4. The equivalent circuit is shown in Fig. 5, where the parasitic capacitances of the drivers have been removed. We call the capacitive network of Fig. 5 the *lumped energy-equivalent DSM bus model*.

Notice that the energy E_i drawn from V_{dd} by the ith driver may be negative! For example, suppose that $\tilde{c}_{1,2}$ is nonzero, that the first line remains connected to V_{dd} during the transition, i.e., $V_1^f = V_1^i = V_{dd}$ and that all other lines transit from zero to V_{dd} i.e., $V_2^i = V_3^i = \cdots = V_n^i = 0$ and $V_2^f = V_3^f = \cdots = V_n^f = $
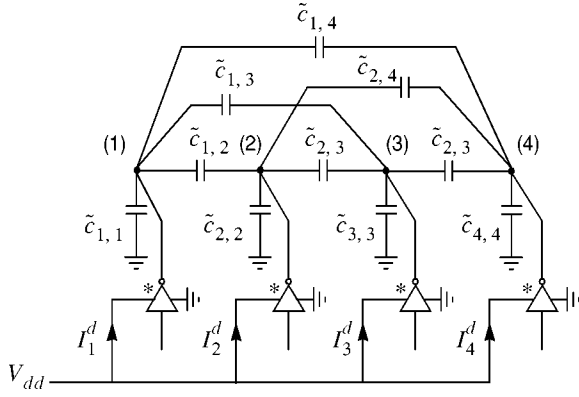
Fig. 5. Energy-equivalent lumped DSM bus model.

Fig. 6. Energy-wise approximate DSM bus model.

Fig. 7. Simple energy-wise approximate DSM bus model.

V_{dd}. Then, current will flow from the first line back to the power supply (Fig. 5).

Although individual drivers may return energy to the power supply, the total energy drawn from it during the transition $E = \sum_{i=1}^{n} E_i$ is always non-negative (Appendix B). Using (16), the total energy E can be written in the form

$$E = (V^f)^T C^t (V^f - V^i). \tag{22}$$

Finally, the model of Fig. 5 can be directly generalized to capture energy losses due to coupling between bus and *nonbus* lines (or lumped nodes). Suppose that the bus has n lines as before and some of them are capacitively (and possibly inductively) coupled to m other nonbus lines (or lumped nodes). We can expand the model of Fig. 5 by adding m more nodes. Under assumptions on the transitions of the voltages of the additional lines (or nodes) similar to that of Section II-B, we can define the expanded vectors of initial and final voltages V^i and V^f, respectively. They both have $n + m$ coordinates, the first n of which correspond to bus lines. The matrix C^t must be expanded appropriately. Then, the energy drawn during the transition from the power supply by the bus drivers is

$$E = \sum_{i=1}^{n} V_i^f e_i^T C^t (V^f - V^i). \tag{23}$$

Note that here e_i has $n + m$ coordinates.

IV. SIMPLIFIED ENERGY-EQUIVALENT MODEL

Traditionally, the bus lines are laid parallel and coplanar. In this case, most of the electric field is trapped between the adjacent lines and the ground. This implies that the capacitance between nonadjacent lines is practically negligible with respect to the capacitance between adjacent lines or the capacitance between the lines and ground. Therefore, an approximate energy-equivalent bus model can ignore the parasitics between nonadjacent lines [15], [19], [22], [25]. In this case, the triplet, drivers-lines-receivers behaves energy wise as the network of Fig. 6, and the matrix C^t is reduced to the tri-diagonal matrix, as seen in the equation at the bottom of the next page. This model can be further simplified if we assume that all grounded capacitors have the same values, except perhaps of the boundary
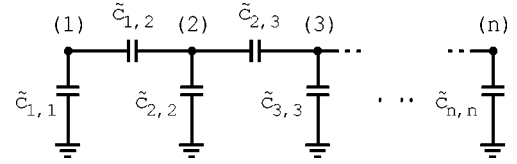
ones (due to fringing effects), and that all the interline capacitances are also of the same value. Say, $\tilde{c}_{2,2} = \tilde{c}_{3,3} = \cdots = \tilde{c}_{n-1,n-1} = C_L$ (subscript L for line capacitance) and $\tilde{c}_{1,2} = \tilde{c}_{2,3} = \cdots = \tilde{c}_{n-1,n} = C_I$ (subscript I for interline). Finally, $\tilde{c}_{1,1} = \tilde{c}_{n,n} = C_L + C_F$ (subscript F for fringing). (Note that by definition, C_L includes the capacitances of the driver and receiver). In this case, the approximate model is as in Fig. 7, and C^t becomes C^{ta} (a for approximate) as in (24)

$$C^{ta} = \begin{bmatrix} 1+\lambda+\zeta & -\lambda & 0 & \cdots & 0 \\ -\lambda & 1+2\lambda & -\lambda & \cdots & 0 \\ 0 & -\lambda & 1+2\lambda & \cdots & 0 \\ \vdots & \vdots & \vdots & \ddots & \vdots \\ 0 & 0 & 0 & \cdots & 1+\lambda+\zeta \end{bmatrix} C_L \tag{24}$$

where we have set

$$\lambda = \frac{C_I}{C_L}, \quad \zeta = \frac{C_F}{C_L}. \tag{25}$$

The parameters λ and ζ depend on the technology as well as the specific geometry, metal layer, and shielding of the bus. In general, ζ is between zero and λ. The parameter λ tends to increase with technology scaling. For standard 0.18-μm technologies and minimum distance between the wires, λ is between 3 and 6, depending on the metal layer. It is expected to be even larger in 0.13 μm. For wide buses, the C_F (or ζ) terms can be ignored since they do not contribute significantly to the total energy consumption.

V. SPICE SIMULATIONS

To verify the simplified model of Fig. 7, a three-line bus along with its drivers, has been designed and simulated using HSPICE. In the design, 0.18-μm technology was used, and the wires had minimal distance to each other and a length of 2 mm. The technology file gave $\lambda = 5.06$ (for metal layer 1). The normalized energies measured using HSPICE simulation, as well as the theoretical ones calculated using the expression $E = V^f C^{ta} (V^f - V^i)$ (with $\zeta = 0$), are shown in Table I. For every transition, the upper number is the HSPICE measurement and the lower one is the calculated value. The variations are within 5.2% and are mostly due to numerical errors in the energy integration.

TABLE I
NORMALIZED ENERGY DRAWN FROM V_{dd} DURING THE TRANSITIONS OF A THREE-LINE DSM BUS WITH $\lambda = 5.06$ (SIMULATION: UPPER/MODEL: LOWER)

(V_1^f, V_2^f, V_3^f)

E (V_1^i, V_2^i, V_3^i)	000	001	010	011	100	101	110	111
000	0	6.02	11.3	6.97	6.02	12.0	6.97	3.14
	0	6.07	11.1	7.07	6.07	12.1	7.07	3.00
001	0	0	16.0	6.00	6.03	6.02	12.0	1.91
	0	0	16.2	6.07	6.07	6.07	12.1	2.00
010	0	11.1	0	0.96	11.1	21.4	0.96	2.10
	0	11.1	0	1.00	11.1	22.3	1.00	2.00
011	0	5.06	5.06	0	11.1	16.1	6.02	0.96
	0	5.07	5.07	0	11.1	16.2	6.07	1.00
100	0	6.02	16.1	12.0	0	6.02	6.00	1.92
	0	6.07	16.2	12.1	0	6.07	6.07	2.00
101	0	0	20.6	11.0	0	0	11.0	0.96
	0	0	21.3	11.1	0	0	11.1	1.00
110	0	11.1	5.06	6.03	5.06	16.1	0	0.96
	0	11.1	5.07	6.07	5.07	16.2	0	1.00
111	0	5.07	10.1	5.06	5.07	10.1	5.06	0
	0	5.07	10.1	5.07	5.07	10.1	5.07	0

Fig. 8. The standard model used for comparison.

TABLE II
NORMALIZED TRANSITION ENERGY DRAWN FROM V_{dd} ESTIMATED USING THE DSM ($\lambda = 3$) (UPPER) AND THE STANDARD (LOWER) MODEL

(V_1^f, V_2^f, V_3^f)

E (V_1^i, V_2^i, V_3^i)	000	001	010	011	100	101	110	111
000	0	4	7	5	4	8	5	3
	0	4	7	11	4	8	11	15
001	0	0	10	4	4	4	8	2
	0	0	7	7	4	4	11	11
010	0	7	0	1	7	14	1	2
	0	4	0	4	4	8	4	8
011	0	3	3	0	7	10	4	1
	0	0	0	0	4	4	4	4
100	0	4	10	8	0	4	4	2
	0	4	7	11	0	4	7	11
101	0	0	13	7	0	0	7	1
	0	0	7	7	0	0	7	7
110	0	7	3	4	3	10	0	1
	0	4	0	4	0	4	0	4
111	0	3	6	3	3	6	3	0
	0	0	0	0	0	0	0	0

VI. DSM VERSUS STANDARD BUS MODEL

In this section, the simple DSM bus model of Fig. 7 is compared energy-wise to the standard bus model in Fig. 8. The standard model has been used and is being used extensively for energy estimation. Although it is convenient for theoretical analysis, it gives misleading results for submicron technology buses.

A. Energy Comparison

In Table II, we see the behavioral differences between the DSM and the standard energy models. It shows the energy drawn from V_{dd} during the different transitions as it was estimated by the two models (Figs. 7 and 8) for the case of a three-line bus $n = 3$ with $\lambda = 3$. For a fair comparison of the two models, the capacitances of the standard bus were set to $C_s = C_L + 2C_I$ and $C_s' = C_L + C_I$. The supply voltage V_{dd} and the line-to-ground capacitance C_L have been normalized to one, and it was assumed that $\zeta = 0$. The upper numbers correspond to the DSM model and the lower ones to the standard model. There is difference not only in the average energy but, most importantly, in the pattern of energy consumption. Some transitions are relatively much more expensive according to one model than the other one. These large differences are due
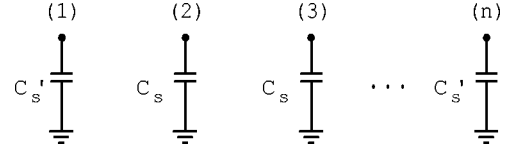
to the interaction between the lines that is captured only by the DSM model. To illustrate this, let i be an intermediate line of the bus. Replacing C^t by C^{ta} in (16), we get

$$E_i = V_i^f e_i^T C^{ta}(V^f - V^i)$$
$$= V_i^f [-\lambda, 1 + 2\lambda, -\lambda] \begin{bmatrix} V_{i-1}^f - V_{i-1}^i \\ V_i^f - V_i^i \\ V_{i+1}^f - V_{i+1}^i \end{bmatrix} C_L. \quad (26)$$

Depending on the values of V_{i-1}^i, V_{i-1}^f, V_i^i, V_i^f, V_{i+1}^i, and V_{i+1}^f, the energy E_i can take the values -2λ, $-\lambda$, 0, λ, 2λ, 1, $1 + \lambda$, $1 + 2\lambda$, $1 + 3\lambda$, or $1 + 4\lambda$ (times $V_{dd}^2 C_L$). On the contrary, for the standard model, it is $E_i = V_i^f C_s(V_i^f - V_i^i)$, which gives the possible values 0 and $1 + 2\lambda$ (times $V_{dd}^2 C_L$). Fig. 9 shows the histograms of the energies calculated with the standard and DSM models for the cases of $n = 3$ and $n = 8$ and with $\lambda = 3$.

$$C^t = \begin{bmatrix} \tilde{c}_{1,1} + \tilde{c}_{1,2} & -\tilde{c}_{1,2} & 0 & \cdots & 0 & 0 \\ -\tilde{c}_{1,2} & \tilde{c}_{1,2} + \tilde{c}_{2,2} + \tilde{c}_{2,3} & -\tilde{c}_{2,3} & \cdots & 0 & 0 \\ 0 & -\tilde{c}_{2,3} & \tilde{c}_{2,3} + \tilde{c}_{3,3} + \tilde{c}_{3,4} & \cdots & 0 & 0 \\ \vdots & \vdots & \vdots & \ddots & \vdots & \vdots \\ 0 & 0 & 0 & \cdots & \tilde{c}_{n-2,n-1} + \tilde{c}_{n-1,n-1} + \tilde{c}_{n-1,n} & -\tilde{c}_{n-1,n} \\ 0 & 0 & 0 & \cdots & -\tilde{c}_{n-1,n} & \tilde{c}_{n-1,n} + \tilde{c}_{n,n} \end{bmatrix}.$$
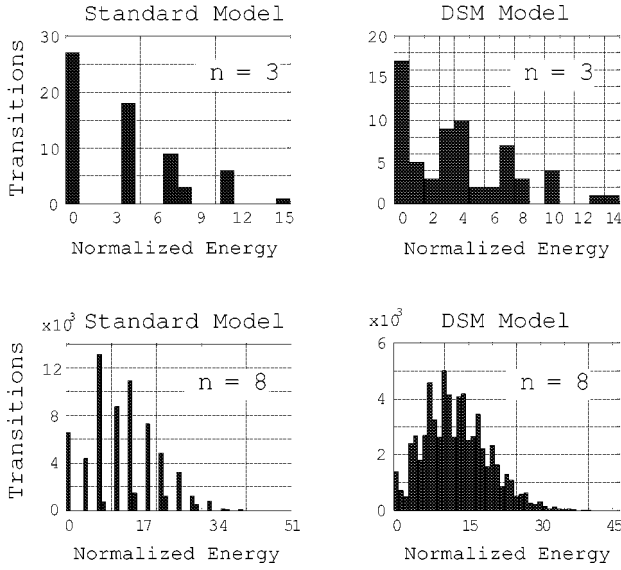
Fig. 9.   Energy histograms based on the standard and DSM ($\lambda = 3$) energy models.

VII. Energy Distribution and Statistical Energy Behavior of DSM Buses

The purpose of this section is twofold. First, the energy formula (22) is utilized to reveal how the energy drawn from V_{dd} is distributed in a bus, i.e., how much energy is (re)stored in the capacitors and how much is dissipated on the resistors. Second, the statistical average energy consumption of the bus is evaluated when the bus is driven by sequences of random data. This is done with the definition of the *transition activity matrix*, a generalization of the *transition activities* of individual lines.

A. Distribution of the Energy Drawn From Vdd

Let $V_1, V_2, \ldots, V_n$ be the voltages along the lines. The energy E_c stored in all the capacitances in the drivers, bus, and receivers can be calculated using the lumped bus model of Fig. 4. It is

$$E_c = \frac{1}{2}\sum_{i=1}^{n} \tilde{c}_{i,i} V_i^2 + \frac{1}{2}\sum_{i<j} \tilde{c}_{i,j}(V_i - V_j)^2$$

or in vector form [using (20)]

$$E_c = \frac{1}{2} V^T C^t V \tag{27}$$

where $V = [V_1, V_2, \ldots, V_n]^T$.

In the beginning of the transition, $t = 0$, the lines have their initial voltages, $V^i = [V_1^i, V_2^i, \ldots, V_n^i]^T$ and so the stored energy is

$$E_c^i = \frac{1}{2}(V^i)^T C^t V^i. \tag{28}$$

At the end of the transition period, $t = T$, the lines have their final voltages $V^f = [V_1^f, V_2^f, \ldots, V_n^f]^T$ and so the stored energy is

$$E_c^f = \frac{1}{2}(V^f)^T C^t V^f. \tag{29}$$

The difference of the two values, $\Delta E_c = E_c^f - E_c^i$, is the energy transferred from the power supply to the capacitors. Through energy conservation

$$E = E_r + \Delta E_c \tag{30}$$

where E_r is the energy dissipated in the drivers and the distributed resistance of the lines. From (22), (28)–(30) we have

$$\begin{aligned}
E_r &= E - \Delta E_c = E - \left(E_c^f - E_c^i\right) \\
&= (V^f)^T C^t (V^f - V^i) - \frac{1}{2}(V^f)^T C^t V^f + \frac{1}{2}(V^i)^T C^t V^i \\
&= \frac{1}{2}(V^f)^T C^t V^f + \frac{1}{2}(V^i)^T C^t V^i - (V^f)^T C^t V^i.
\end{aligned} \tag{31}$$

The matrix C^t is symmetric and so the following identity holds

$$(V^f)^T C^t V^i = \frac{1}{2}(V^f)^T C^t V^i + \frac{1}{2}(V^i)^T C^t V^f.$$

Therefore, from (31), the dissipated energy (transformed into heat) is

$$\boldsymbol{E_r = \frac{1}{2}(V^f - V^i)^T C^t (V^f - V^i).} \tag{32}$$

The right side of (32) is a positive definite quadratic form since C^t is a positive definite matrix (assuming no $c_{i,i}^t$ is zero). It is also a generalization of the classic expression $E = cv^2/2$ and can replace (22) when long term average energy has to be estimated. To see this, suppose the bus is driven by a finite sequence of data corresponding to the sequence of voltage vectors $V(0), V(1), \ldots, V(m)$. There are m transitions and by (22) the *average energy drawn from V_{dd} per transition* is

$$\overline{E} = \frac{1}{m}\sum_{k=1}^{m} V^T(k) C^t \left(V(k) - V(k-1)\right). \tag{33}$$

From (32) the average energy dissipated on the resistors per transition is

$$\overline{E_r} = \frac{1}{m}\sum_{k=1}^{m} \frac{(V(k) - V(k-1))^T C^t (V(k) - V(k-1))}{2}. \tag{34}$$

By expanding (33) and (34) we get

$$\overline{E_r} = \overline{E} + \frac{V^T(0) C^t V(0) - V^T(m) C^t V(m)}{2m} \tag{35}$$

and so $\overline{E}$ and $\overline{E_r}$ become asymptotically equal as $m \to \infty$.

B. Expected Energy – The Transition Activity Matrix

The standard model has given rise to the transition activities of the lines. Let $l_i(1), l_i(2), \ldots$ be a sequence of bits transmitted through the ith line. For the kth transition we have, $V_i^i(k) = V_{dd} l_i(k)$ and $V_i^f(k) = V_{dd} l_i(k+1)$. Then, according to the standard model (Fig. 7 with $C_I = C_F = 0$), the energy drawn from the power supply by the driver of the ith line is

$$E_i(k) = l_i(k+1)\left[l_i(k+1) - l_i(k)\right] V_{dd}^2 C_L. \tag{36}$$

If the random data sequence $\{l_i(k)\}_k$ is stationary with the wide sense, its autocorrelation function is defined as

$$R_i(r) = \mathcal{E}\left[l_i(k)l_i(k+r)\right] \tag{37}$$

where $\mathcal{E}$ stands for expectation. Then, the *expected energy per transition drawn by the ith driver* can be expressed as

$$\mathcal{E}\left[E_i(k)\right] = \left[R_i(0) - R_i(1)\right]V_{dd}^2 C_L. \tag{38}$$

The factor

$$a_i = R_i(0) - R_i(1) \tag{39}$$

is called the *transition activity* of the ith line. So

$$\mathcal{E}\left[E_i(k)\right] = a_i V_{dd}^2 C_L. \tag{40}$$

According to the standard model (Fig. 7 with $C_I = C_F = 0$), the expected energy per cycle drawn by the whole bus is

$$\mathcal{E}\left[E_i(k)\right] = \left\{\sum_{i=1}^{n} a_i\right\} V_{dd}^2 C_L. \tag{41}$$

In the standard model, the energy drawn by a line is independent of the data transmitted on the other lines. This is not true for the DSM bus model. Transition activity on a line influences the adjacent lines as well.

Again, let $\{l_i(k)\}_k$, be the random bit sequences on the lines $i = 1, 2, \ldots, n$, respectively. Here we assume the sequences are jointly wide sense stationary. Let

$$R_{i,j}(r) = \mathcal{E}\left[l_i(k)l_j(k+r)\right] \tag{42}$$

be the cross correlation of the sequences i and j. We can define the sequence of random vectors $L(k) = [l_1(k), l_2(k), \ldots, l_n(k)]^T$ and its autocorrelation matrix

$$R(r) = [R_{i,j}(r)]_{i,j=1}^{n} = \mathcal{E}\left[L(k)L^T(k+r)\right]. \tag{43}$$

The voltages of the lines follow their binary values, $V(k) = V_{dd}L(k)$. For the kth transition we have that

$$\begin{aligned}
E(k) &= V^T(k+1)C^t[V(k+1) - V(k)]\\
&= \mathrm{tr}\left\{V^T(k+1)C^t[V(k+1) - V(k)]\right\}\\
&= \mathrm{tr}\left\{C^t\left[V(k+1)V^T(k+1) - V(k)V^T(k+1)\right]\right\}
\end{aligned} \tag{44}$$

where $\mathrm{tr}(X)$ is the trace of matrix X. In (44) we used the identity [31]

$$\mathrm{tr}(XY) = \mathrm{tr}(YX). \tag{45}$$

From (43) and (44) we get

$$\mathcal{E}\left[E(k)\right] = V_{dd}^2 \,\mathrm{tr}\left\{C^t[R(0) - R(1)]\right\}. \tag{46}$$

The similarity between (41) and (46) becomes clear if we rewrite (41) as

$$\mathcal{E}\left[E(k)\right] = V_{dd}^2 \,\mathrm{tr}\left\{\mathcal{I} \cdot C_L[R(0) - R(1)]\right\}$$

where $\mathcal{I}$ is the identity matrix. Identity (45) along with the symmetry of C^t and the fact that $\mathrm{tr}(A) = \mathrm{tr}(A^T)$ imply that

$$\mathrm{tr}\left\{C^t R(1)\right\} = \mathrm{tr}\left\{R^T(1)\left(C^t\right)^T\right\} = \mathrm{tr}\left\{C^t R^T(1)\right\}. \tag{47}$$

Equation (47) allows us to write (46) in the following symmetric form:

$$\mathcal{E}\left[E(k)\right] = V_{dd}^2 \,\mathrm{tr}\left\{C^t\left[R(0) - \frac{R(1) + R^T(1)}{2}\right]\right\}. \tag{48}$$

We define the *transition activity matrix* $\mathcal{A}$ as

$$\mathcal{A} = R(0) - \frac{R(1) + R^T(1)}{2} \tag{49}$$

the elements of which are

$$\begin{aligned}
a_{i,j} &= R_{i,j}(0) - \frac{[R_{i,j}(1) + R_{j,i}(1)]}{2}\\
&= \mathcal{E}\left[l_i(k)l_j(k)\right] - \frac{\mathcal{E}\left[l_i(k)l_j(k+1) + l_j(k)l_i(k+1)\right]}{2}.
\end{aligned} \tag{50}$$

The transition activity matrix $\mathcal{A}$ is symmetric by its definition. This was done so because both the cross activities $a_{i,j}$ and $a_{j,i}$ express the interaction between the lines i and j. The transition activity matrix is also positive definite [31] (for nondegenerate statistics). To see this, we use the stationarity of $\{L(k)\}_k$ to write $\mathcal{A}$ as

$$\mathcal{A} = \frac{1}{2}\mathcal{E}\left[(L(k+1) - L(k))(L(k+1) - L(k))^T\right].$$

The definition of the transition activity matrix is in agreement with the standard definition of transition activities of the lines. From (39) and (50), it is $a_i = a_{i,i}$. Finally, expression (48) is written as

$$\mathcal{E}\left[E(k)\right] = V_{dd}^2 \,\mathrm{tr}\left\{C^t \mathcal{A}\right\}. \tag{51}$$

A simpler form for the expected energy can be found if we replace C^t in (51) by its approximation C^{ta}. In this case, we have

$$\begin{aligned}
\mathcal{E}\left[E(k)\right] &= V_{dd}^2 \,\mathrm{tr}\left\{C^{ta}\mathcal{A}\right\}\\
&= \left\{(1 + \lambda + \zeta)(a_{1,1} + a_{n,n})\right.\\
&\quad \left. + (1 + 2\lambda)\sum_{i=2}^{n-1} a_i - 2\lambda\sum_{i=1}^{n-1} a_{i,i+1}\right\} V_{dd}^2 C_L.
\end{aligned}$$

The above expression can be further simplified if we make the approximation $\zeta = \lambda$

$$\mathcal{E}\left[E(k)\right] = \left\{(1 + 2\lambda)\sum_{i=1}^{n} a_i - 2\lambda\sum_{i=1}^{n-1} a_{i,i+1}\right\} V_{dd}^2 C_L$$

C. Example: Uniformly Distributed, IID Data

A common assumption in energy estimation is that the data sequences are sequences of specially and temporally independent random bits with uniform distribution. In other words, that the random bits

$$l_1(1), l_2(1), \ldots, l_n(1), l_1(2), l_2(2), \ldots, l_n(2), \ldots$$

are independent random variables s.t.

$$P_r(l_i(k) = 0) = P_r(l_i(k) = 1) = 1/2$$

for all i and k. Then

$$\mathcal{E}\left[l_i(k)l_j(k+r)\right] = \begin{cases} \frac{1}{2} & \text{if } i = j \text{ and } r = 0 \\ \frac{1}{4}, & \text{otherwise} \end{cases}.$$

The transition activity matrix is $\mathcal{A} = 1/4\mathcal{I}$ and the expected energy is

$$\mathcal{E}\left[E(k)\right] = \left\{\frac{n}{4} + \frac{n-1}{2}\lambda + \frac{\zeta}{2}\right\} V_{dd}^2 C_L$$

VIII. CONCLUSION

A DSM bus energy model has been introduced and studied. Closed form expressions for the transition energy of this model have been derived. The deterministic and statistical energy behavior of the DSM model have been discussed and compared to that of the simplistic standard bus model. The transition activity matrix has been introduced as a generalization of the transition activities of the lines.

APPENDIX I

To prove (16) we start by replacing (14) into (15)

$$\begin{aligned} E_i &= V_i^f \int_0^T \left\{ I_i(0,t) + C_i^d \frac{\partial V_i(0,t)}{\partial t} \right\} dt \\ &= V_i^f \cdot \int_0^T I_i(0,t)dt + V_i^f C_i^d \int_0^T \frac{\partial V_i(0,t)}{\partial t} dt \\ &= V_i^f \int_0^T I_i(0,t)dt + V_i^f C_i^d \left(V_i^f - V_i^i\right). \end{aligned} \quad (52)$$

Now, we evaluate the time integral of $I_i(0,t)$ using (1). Integration of both sides of (1) on x over $[0, L_p]$ gives

$$I(0,t) = I(L_p,t) + \int_0^{L_p} C(x)\frac{\partial V(x,t)}{\partial t}dx. \quad (53)$$

From Fig. 3, $I_i(L_p,t) = C_i^r(\partial V_i(L_p,t)/\partial t)$, or written in vector form, $I(L_p,t) = C^r(\partial V(L_p,t)/\partial t)$. By replacing the last one into (53) and integrating over the time period we get

$$\begin{aligned} \int_0^T I(0,t) &= \int_0^T C^r \frac{\partial V(L_p,t)}{\partial t}dt \\ &\quad + \int_0^T \left(\int_0^{L_p} C(x)\frac{\partial V(x,t)}{\partial t}dx \right) dt \\ &= C^r(V^f - V^i) + \int_0^T \left(\int_0^{L_p} C(x)\frac{\partial V(x,t)}{\partial t}dx \right) dt. \end{aligned} \quad (54)$$

The matrix function $C(x)\partial V(x,t)/\partial t$ is Lebesgue integrable [30] within $[0, L_p] \times [0, T]$. This allows the use of Fubini's the-

orem [30] and the change of the integration order in the double integral of (54). It is

$$\begin{aligned} \int_0^T &\left(\int_0^{L_p} C(x)\frac{\partial V(x,t)}{\partial t}dx \right) dt \\ &= \int_0^{L_p} \left(\int_0^T C(x)\frac{\partial V(x,t)}{\partial t}dt \right) dx \\ &= \int_0^{L_p} C(x) \left(\int_0^T \frac{\partial V(x,t)}{\partial t}dt \right) dx \\ &= \int_0^{L_p} C(x)(V^f - V^i)dx \\ &= \left(\int_0^{L_p} C(x)dx \right) (V^f - V^i). \end{aligned} \quad (55)$$

Expressions (54) and (55) give

$$\int_0^T I(0,t)dt = \left[C^r + \int_0^{L_p} C(x)dx \right] (V^f - V^i). \quad (56)$$

Since it is $I_i(0,t) = e_i^T I(0,t)$, where e_i has a one in the ith position and zero everywhere else, and since C^d is diagonal, (52) and (56) imply that

$$\begin{aligned} E_i &= V_i^f \int_0^T I_i(0,t)dt + V_i^f C^d(V_i^f - V_i^i) \\ &= V_i^f e_i^T \left[C^r + \int_0^{L_p} C(x)dx \right] (V^f - V^i) \\ &\quad + V_i^f C^d(V_i^f - V_i^i) \\ &= V_i^f e_i^T \left[C^d + C^r + \int_0^{L_p} C(x)dx \right] (V^f - V^i). \end{aligned}$$

We have set $C^t = C^d + C^r + \int_0^{L_p} C(x)dx$ and therefore it is

$$E_i = V_i^f e_i^T C^t (V^f - V^i). \quad (57)$$

APPENDIX II

Here we show that for any transition of the bus, the total energy $E = \sum_{i=1}^n E_i$ is non-negative. Matrix C^t, whose elements are given by (20) can be written as

$$C^t = \begin{bmatrix} \tilde{c}_{1,1} & & \\ & \tilde{c}_{2,2} & 0 \\ & 0 & \ddots \\ & & & \tilde{c}_{n,n} \end{bmatrix} + \sum_{i<j} \left(e_i e_i^T - e_i e_j^T - e_j e_i^T + e_j e_j^T \right) \tilde{c}_{i,j}.$$

Starting from (22) and using the above expression, the transition energy is written as: shown in the equation at the top of the next page. It is easy to verify that $V_i^f(V_i^f - V_i^i) \geq 0$ and $(V_j^f - V_i^f)\left[(V_j^f - V_i^f) - (V_j^i - V_i^i)\right] \geq 0$ for all values of V^i and V^f. Therefore, it is $E \geq 0$.

$$
\begin{aligned}
E =& V^f C^t (V^f - V^i) \\
=& \sum_{i=1}^{n} V_i^f (V_i^f - V_i^i) \tilde{c}_{i,i} + \sum_{i<j} \left\{ V_i^f (V_i^f - V_i^i) + V_j^f (V_j^f - V_j^i) - V_i^f (V_j^f - V_j^i) - V_j^f (V_i^f - V_i^i) \right\} \tilde{c}_{i,j} \\
=& \sum_{i=1}^{n} V_i^f (V_i^f - V_i^i) \tilde{c}_{i,i} + \sum_{i<j} (V_j^f - V_i^f) \left[(V_j^f - V_i^f) - (V_j^i - V_i^i) \right] \tilde{c}_{i,j}.
\end{aligned}
$$

REFERENCES

[1] S. Borkar, "Low power design challenges for the decade," in *Proc. Asia South Pacific Design Automation Conf.*, 2001, pp. 293–296.

[2] T. Sakurai, "Design Challenges for 0.1 μm and Beyond," in *Proc. Asia South Pacific Design Automation Conf.*, 2000, pp. 553–558.

[3] B. Bishop and M. J. Irwin, "Databus charge recovery: Practical considerations," in *Proc. IEEE/ACM Int. Symp. Low Power Electron. Design*, San Diego, CA, 1999, pp. 85–87.

[4] H. Yamauchi, H. Akamatsu, and T. Fujita, "An asymptotically zero power charge-recycling bus architecture for battery-operated ultrahigh data rate ULSI's," *IEEE J. Solid-State Circuits*, pp. 423–431, Apr. 1995.

[5] K. Y. Khoo and A. Willson Jr, "Charge recovery on a databus," in *Proc. IEEE/ACM Int. Symp. Low Power Electron. Design*, New York, 1995, pp. 185–189.

[6] E. Kush and J. Rabaey, "Low-Energy Embedded FPGA Structures," in *IEEE/ACM Int. Symp. Low Power Electron. Design*, Monterey, CA, 1998, pp. 155–160.

[7] P. Sotiriadis, T. Konstantakopoulos, and A. Chandrakasan, "Analysis and Implementation of Charge Recycling for Deep Sub-micron Buses," in *IEEE/ACM Int. Symp. Low Power Electron. Design*, Huntington Beach, CA, 2001, pp. 364–369.

[8] S. Ramprasad, N. Shanbhag, and I. Hajj, "A coding framework for low-power address and data busses," *IEEE Trans. VLSI Syst.*, vol. 7, pp. 212–221, June 1999.

[9] M. Stan and W. Burleson, "Low-power encodings for global communication in CMOS VLSI," *IEEE Trans. VLSI Syst.*, vol. 5, pp. 49–58, Dec. 1997.

[10] P. Sotiriadis and A. Chandrakasan, "Low power bus coding techniques considering inter-wire capacitances," in *Proc. Custom Integrated Circuits Conf. (CICC)*, 2000, pp. 507–510.

[11] ——, "Bus Energy Minimization by Transition Pattern Coding (TPC) in Deep Sub-Micron Technologies," in *Proc. IEEE/ACM Int. Conf. Comput. Aided Design*, 2000, pp. 322–327.

[12] Y. Nakagome, K. Itoh, M. Isoda, K. Takeuchi, and M. Aoki, "Sub 1 V swing internal bus architecture for future low-power ULSI's," *IEEE J. Solid-State Circuits*, vol. 28, pp. 414–419, Apr. 1993.

[13] M. Hiraki, H. Kojima, H. Misawa, T. Akazawa, and Y. Hatano, "Data-dependent logic swing internal bus architecture for ultra low-power LSI's," *IEEE J. Solid-State Circuits*, vol. 30, pp. 397–401, Apr. 1995.

[14] H. Zhang and J. Rabaey, "Low swing interconnect interface circuits," in *Proc. IEEE/ACM Int. Symp. Low Power Electron. Design*, Aug. 1998, pp. 161–166.

[15] J. Davis and J. Meindl, "Compact Distributed RLC Interconnect Models Part II: Coupled Line Transient Expressions and Peak Crosstalk in Multilevel Networks," *IEEE Trans. Electron. Devices*, vol. 47, pp. 2078–2087, Nov. 2000.

[16] K. Yamashita and S. Odanaka, "Interconnect Scaling Scenario Using a Chip Level Interconnect Model," *IEEE Trans. Electron. Devices*, vol. 47, pp. 90–96, Jan. 2000.

[17] N. Menezes and L. Pillegi, "Analyzing on-chips Interconnect effects," in *Design of High Performance Microprocessor Circuits*, 2001 ed, A. Chandrakasan, W. J. Bowhill, and F. Fox, Eds. Piscataway, NJ: IEEE Press, ch. 16.

[18] S. Morton, "Techniques for Driving interconnect," in *Design of High Performance Microprocessor Circuits*, 2001 ed, A. Chandrakasan, W. J. Bowhill, and F. Fox, Eds. Piscataway, NJ: IEEE Press, ch. 17.

[19] S. Das, W. Smith, and C. Paul, "Modeling of data bus structures using numerical methods," in *Proc. Int. Symp. Electromagnetic Compatibility*, Dallas, TX, 1993, pp. 409–414.

[20] A. E. Ruehli, Ed., *Circuit analysis, simulation, and design*. New York: Elsevier, 1986–1987, vol. 1,2.

[21] S. C. Wong, G.-Y. Lee, and D.-J. Ma, "Modeling of Interconnect Capacitance, Delay, and Crosstalk in VLSI," *IEEE Trans. Semiconduct. Manufacturing*, vol. 13, pp. 108–111, Feb. 2000.

[22] C. K. Cheng, J. Lillis, S. Lin, and N. Chang, *Interconnect Analysis and Synthesis*. New York: Wiley, 2000.

[23] L. Pileggi, "Coping with RC(L) interconnect design headaches," in *Proc. IEEE/ACM Int. Conf.*, San Jose, CA, 1995, pp. 246–253.

[24] Y. I. Ismail, E. G. Friedman, and J. L. Neves, "Transient power in CMOS gates driving LC transmission lines," in *Proc. IEEE Int. Conf. Electron. Circuits.Systems*, Lisbon, Portugal, 1998, pp. 337–340.

[25] J. M. Rabaey, *Digital Integrated circuits*. Englewood Cliffs, NJ: Prentice-Hall, 1996.

[26] T. Sakurai, "Closed-form expressions for interconnection delay, coupling, and crosstalk in VLSI's," *IEEE Trans. Electron. Devices*, vol. 40, pp. 118–124, Jan. 1993.

[27] K. T. Tang and E. G. Friedman, "Peak noise prediction in loosely coupled interconnect [VLSI circuits]," in *Proc. Int. Symp. Circuit Syst.*, vol. 1, 1999, pp. 541–544.

[28] T. Sakurai, S. Kobayashi, and M. Noda, "Simple expressions for interconnection delay, coupling and crosstalk in VLSI," in *Proc. Int. Symp. Circuit Syst.*, vol. 4, Singapore, June 1991, pp. 2375–2378.

[29] M. Becer and I. N. Hajj, "An analytical model for delay and crosstalk estimation in interconnects under general switching conditions," *IEEE Int. Electron., Circuits Syst.*, vol. 2, pp. 831–834, Dec. 17–20, 2000.

[30] F. Riesz and B. Nagy, *Functional Analysis*. New York: Dover, 1990.

[31] R. A. Horn and C. R. Johnson, *Matrix Analysis*. Cambridge, U.K.: Cambridge Univ. Press, 1994.

[32] A. Ruehli, "Equivalent Circuit Models for Three-Dimensional Multiconductor Systems," *IEEE Trans. Microwave Theory Tech.*, vol. MTT-22, pp. 216–221, Mar. 1974.

Paul P. Sotiriadis received the Diploma degree in electrical engineering from the National Technical University of Athens (NTUA), Greece, with highest honors, in 1994, and the MSEE degree from Stanford University, Palo Alto, CA, in 1996. He is currently working toward the Ph.D. degree in the Department of Electrical Engineering and Computer Sciences, Massachusetts Institute of Technology, Cambridge.

His main research interests include low-power circuit design, signal processing, and related mathematical problems.

Mr. Sotiriadis received the Hellenic Mathematical Society Distinction in 1988; the NTUA Department of Mathematics Distinction in 1990; the annual Technical Chamber of Greece award from 1990 to 1994; and the Hellenic Scholarship Foundation Award from 1990 to 1994.

Anantha P. Chandrakasan (S'87–M'95–SM'01) received the B.S., M.S., and Ph.D. degrees in electrical engineering and computer sciences from the University of California, Berkeley, in 1989, 1990, and 1994, respectively.

In September 1994, he joined the Massachusetts Institute of Technology (MIT), Cambridge, where he is currently an Associate Professor of electrical engineering and computer science. From 1994 to 1997, he held the Analog Devices Career Development Chair and received the NSF Career Development Award in 1995, the IBM Faculty Development Award in 1995, and the National Semiconductor Faculty Development award in 1996 and 1997 from MIT. His research interests include the ultra-low-power implementation of custom and programmable digital signal processors, distributed wireless sensors, multimedia devices, emerging technologies, and CAD tools for VLSI. He is a coauthor of *Low Power Digital CMOS Design* (Norwell, MAJ: Kluwer) and a coeditor of *Low Power CMOS Design* (Piscataway, NJ: IEEE Press, 1995) and *Design of High-Performance Microprocessor Circuits* (Piscataway, NJ: IEEE press, 2000).

Dr. Chandrakasan has served on technical program committees of various conferences including ISSCC, VLSI Circuits Symposium, DAC, and the international Symposium on Low-power Electronics and Design (ISLPED). He served as a Technical Program Cochair for the 1997 ISLPED, the 1998 VLSI Design Conference, for the 1998 IEEE Workshop on Signal Processing Systems; and he served as a General Cochair of the 1998 ISLPED. He received the 1993 IEEE Communications Society's Best Tutorial Paper Award, the IEEE Electron Devices Society's Paul Rappaport Award for the Best Paper in an EDS publication during the 1997 and 1999 Design Automation Conference Design Contest Award. From 1998 to 2001, he was an Associate Editor for the IEEE JOURNAL OF SOLID-STATE CIRCUITS. He served as an elected Member of the Design and Implementation of Signal Processing Systems (DISPS) Technical Committee of the Signal Processing Society. From 1999 to 2001, he was the Signal Subcommittee Chair for ISSCC; in 2002, he was Vice-Chair and in 2003, he will be Technical Program Chair.